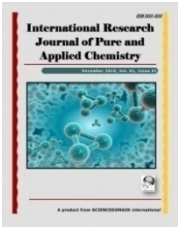

International Research Journal of Pure & Applied Chemistry
5(1): 30-42, 2015, Article no.IRJPAC.2015.004
ISSN: 2231-3443

SCIENCEDOMAIN *international*
www.sciencedomain.org

Synthesis, Characterization and Electrochemical Studies on $Li_4Fe(CN)_6$ as Cathode Material for Lithium Batteries

Bikash Mandal[1], I. Basumallick[1] and Susanta Ghosh[2*]

[1]Electrochemistry Laboratory, Department of Chemistry, Visva-Bharati University, Santiniketan-731235. India.
[2]Electrochemistry Laboratory, Integrated Science Education and Research Centre, Visva-Bharati University, Santiniketan-731235, India.

Authors' contributions

This work was carried out in collaboration between all authors. All authors read and approved the final manuscript.

Article Information

DOI: 10.9734/IRJPAC/2015/10924
Editor(s):
(1) Luigi Campanella, Head, Research Centre on Environment and Cultural Heritage Chemistry, University of Rome "La Sapienza", Piazzale Aldo Moro, 5 00185 Rome, Italy.
(2) Ichiro Imae, Division of Chemistry and Chemical Engineering, Faculty of Engineering, Hiroshima University, Japan.
Reviewers:
(1) Anonymous, Jain University, India.
(2) L. Z. Pei, School of Materials Science and Engineering, Anhui Universit of Technology, P. R. China.
(3) Anonymous, Institute of Metal Research, China.
(4) Anonymous, Xi'an Jiaotong University, China.
(5) Anonymous, Hunan University, China.
(6) Anonymous, University of Tsukuba, Japan
(7) Anonymous, Jazan University, Saudi Arabia.
Complete Peer review History: http://www.sciencedomain.org/review-history.php?iid=650&id=7&aid=6397

Original Research Article

Received 16th April 2014
Accepted 22nd July 2014
Published 8th October 2014

ABSTRACT

An easy and cost effective method of synthesis of $Li_4Fe(CN)_6$ has been reported. The material, as obtained, has been characterized by UV-VIS, FTIR, powder XRD and SEM-EDX. Cyclic-voltametry and charge-discharge studies were carried out for electrochemical characterization of the synthesized material. A laboratory model lithium cell was fabricated using $Li_4Fe(CN)_6$ as cathode, lithium metal as anode and 1M $LiClO_4$ dissolved in ethylene carbonate and dimethyl carbonate (1:1) mixture as electrolyte. The cell shows an open circuit voltage (OCV) of 3.03 volts vs. Li and a discharge capacity of 90 $mAhg^{-1}$ (theoretical capacity, 112 $mAhg^{-1}$) in the first few cycles at 0.15 C

**Corresponding author: Email: susanta.ghosh@visva-bharati.ac.in;*

rates. The charge-discharge behaviour remains practically unaltered up to 20 cycles. Thus $Li_4Fe(CN)_6$ may be considered as a promising cathode material for Lithium battery.

Keywords: $Li_4Fe(CN)_6$ cathode; cost effective method; low temperature calcinations; charge-discharge; lithium battery.

1. INTRODUCTION

Lithium-ion batteries are one of the most powerful [1], and popular storage systems due to highest energy-to-weight ratios, no memory effect, and slight energy loss when not in use [2]. Beyond consumer electronics, lithium-ion batteries are being used for military, electric vehicles and aerospace applications because it has the greatest electrochemical potential and provides the largest energy density, 125-150 $Whkg^{-1}$ [1].

Commercial lithium-ion batteries contain $LiCoO_2$ as the cathode material, in which the component element cobalt is very expensive and toxic [3,4]. As a result large scale applications using this material are limited. Therefore, scientists are looking for new cathode materials, which are less expensive and compatible with the environment [4]. During last decade, a number of new cathode materials were proposed. However, none of them are found suitable for commercial applications due to different critical issues, such as toxicity, higher resistivity, smaller specific capacity, low operating potential, lower cyclibility and large capacity fading upon cycling. Among them layered $LiMnO_2$ and spinel $LiMn_2O_4$ compounds have been drawn more attention as alternative cathode materials for lithium-ion batteries [5-10]. But it has low diffusion co-efficient of lithium-ion and large capacity fading upon cycling.

Recently, lithium iron phosphate ($LiFePO_4$) become an attractive alternating cathode material for rechargeable lithium-ion batteries [11-16], due to low cost starting materials, environment friendly, excellent cycling performances, high theoretical capacity (170 $mAhg^{-1}$), high safety, good operating voltage and high temperature performance [2,11-14]. Again the main disadvantage associated with this material is its low electronic conductivity and low diffusion coefficient of lithium ions, which lead to its poor rate capability [13,14]. Some efforts to increase its conductivity have been made after doping with higher valence metal cations, like Ti^{4+}, Ga^{3+}, Zr^{4+}, W^{6+}, V^{3+} etc. and a few fold enhancements in conductivity is reported in the cost of its intrinsic capacity [17-20]. It will be interesting to increase the conductivity without losing its capacity and that can be done by synthesizing nano $LiFePO_4$ through different particle size controlled techniques like water-based [21-26], sol-gel [27-30], sonochemical [31], solvothermal [32], ionothermal [33], and in-situ carbon coating via solid-state synthetic method [34]. Most of the reported methods are lengthy and expensive. There are few reports available on the synthesis of nano $LiFePO_4$ [16,24,25,31], over large surface area carbon powder with better performance and cyclibility.

However, it is very much difficult to synthesize pure $LiFePO_4$ via solid state or sol-gel methods, because these methods require an inert atmosphere during calcinations to protect oxidation of Fe^{2+} to Fe^{3+} [11-20]. Therefore nitrogen or argon gas and an instrumental set up are required to make inert atmosphere which is costly, and difficult to achieve.

Here, we report a new cathode material $Li_4Fe(CN)_6$ [35], which is synthesized in a simple route without using inert atmosphere and high temperature calcinations [15-25]. Material retains its discharge capacity close to its theoretical value 112 $mAhg^{-1}$, which is slightly lower than the commercial material [36]. On the other hand, $Li_4Fe(CN)_6$ is soluble in water, and thus it can be used as liquid cathode [37], in aqueous lithium-ion battery.

2. MATERIALS AND METHODS

2.1 Material Synthesis Procedure

Concentrated solutions of $K_4Fe(CN)_6.3H_2O$ (BDH, USA, 99%) (6 g in 25 ml) and $LiClO_4$ (Alfa-Aesar, USA, 99%) (6.045 g in 15 ml) were prepared separately. They were then mixed together at room temperature under constant stirring condition. A white crystalline precipitate of $KClO_4$ was appeared (because the solubility of $KClO_4$ in water is 1.5 g/100 ml at 25ºC [38]. The precipitate was filtered and the filtrate was cooled down to 10ºC and kept overnight. Another layer of white precipitate of $KClO_4$ was appeared, which was collected by filtration and the remaining solution was concentrated by evaporating the water at a temperature of 60-70ºC with the help of vacuum evaporator. Then concentrated solution was cooled down to 10ºC and left for 12 hours. Again a crystalline precipitate of $KClO_4$ was appeared. The precipitate was filtered out and the process was

repeated to remove $KClO_4$ completely. The filtrate containing $Li_4Fe(CN)_6$ was then evaporated to dryness and sintered at a temperature of 180ºC. Now the synthesized anhydrous material was cooled down to room temperature and kept in a sealed moisture free bottle for further analysis.

2.2 Characterization Part

Thermo-gravimetric analysis of the solid material, obtained after dehydration of filtrate containing $Li_4Fe(CN)_6$, was made using a Perkin-Elmer TGA/DTA thermal analyzer in nitrogen atmosphere at a heating rate of 20ºCmin^{-1}.

$Li_4Fe(CN)_6$ was characterized by UV-Visible spectroscopy (OPTIZEN POP), Fourier Transform Infrared (FTIR, FTIR-8400S, Shimadzu, Japan), Scanning Electron Microscopy (SEM) and Energy-dispersive X-ray spectroscopy (EDX) (SEM-EDX, JEOL, JSM-6360, UK).

Powder XRD patterns of $K_4Fe(CN)_6.3H_2O$, $K_4Fe(CN)_6$, $K_3Fe(CN)_6$, $KClO_4$, and $Li_4Fe(CN)_6$ were recorded (XRD, Ultima III Rigaku Cu Kα, λ=1.5406 Å) in the range of 2θ=10º-70º with scan rate of 5ºmin^{-1}. $K_4Fe(CN)_6$ was prepared by heating $K_4Fe(CN)_6$. $3H_2O$ (BDH, USA, 99%) at 200ºC for 4 hours; $KClO_4$ was collected as the byproduct during synthesis of $Li_4Fe(CN)_6$ and $K_3Fe(CN)_6$ (BDH, USA, 99%) was obtained commercially.

Cyclic-voltametry and Charge-discharge studies were carried out by a Galvanostat/Potentiostat (VersaStat™II, Princeton Applied Research). The reversibility and the storage capacity of the synthesized material were studied by cyclic-voltametry and chrono-amperometry studies, respectively after preparing a laboratory model cell. The cathode mixture was prepared by mixing the synthesized material (80 wt %) with carbon conductive additive i.e., carbon black (Alfa Aesar, USA, 99.9%) (8 wt %), graphite powder (Alfa Aesar, USA, 99.99%) (8 wt %) and Polyvinylidene fluoride (Aldrich, USA) (4 wt %) binder in N-methyl pyrrolidone (Merck, USA, 99.5%) as solvent to make homogeneous slurry [26-34]. Spherical shaped, nanosized carbon black increases electronic conductivity throughout the active cathode material making contact with the particles. Whereas, platelet-like shaped having lower specific surface area graphite powder not only serves as a good conductor, but like a lubricant also [39,40].The lubricating nature of the platelet graphite create new surface area and provide more contact with the active particles during the ball-milling process, whereas the spherical nanosized carbon black self-agglomerates. Combination of these two types of carbon controls the homogeneity of the mixture, porosity of the cathode, and consequently, the overall conductivity, which affects the cell performance. The slurry, as obtained, was next spread over a thin aluminum foil using a doctor blade so that they are uniformly distributed. N-methyl pyrrolidone and moisture was removed by heating the foil at 80ºC with the help of a vacuum evaporator. The positive electrode was ready for cell fabrication upon cooling down to room temperature. Li (Aldrich, USA, 99.9%) ribbon pasted on a nickel plate was used as anode. One molar $LiClO_4$ (Alfa Aesar, 99%) dissolved in 1:1 mixture of Ethylene carbonate (EC) (Sigma-Aldrich, USA, 98%) and Dimethyl carbonate (DMC) (Sigma-Aldrich, USA, 99%) and porous polypropylene (PP) film soaked with this electrolyte, was used as electrolyte and separator, respectively. The cell was assembled inside a glove bag after removing air and moisture by purging argon gas.

3. RESULTS AND DISCUSSION

3.1 Thermal Gravimetric Analysis (TGA)

Fig. 1 presents the TGA curve of the percentage weight loss vs. temperature of $Li_4Fe(CN)_6$.From the figure, it is clear that there is a weight gain within 60ºC and this might be due to adsorption of carrier gas nitrogen or moisture. Afterwards a weight loss ~4.7% occurred due to loss of adsorbed moisture within 120ºC. Above this temperature up to 350ºC another 3.1% weight loss occurred due to removal of crystal water from $Li_4Fe(CN)_6$. Above this temperature, weight loss occurred stepwise due to decomposition of the compound. Therefore, sintering the material within 180ºC can produce dehydrated material because within this temperature the material does not decompose, but undergoes dehydration only.

3.2 UV-Visible Spectroscopy

The UV-Visible spectrum of aqueous solution containing $Li_4Fe(CN)_6$ is shown in Fig. 2.

From Fig. 2, it is found that an intense absorption peak at 220 nm, attributed to the presence of ferrocyanide group which overlaps with absorption maxima of the commercial $K_4Fe(CN)_6.3H_2O$ crystals. This suggest that the material, obtained after

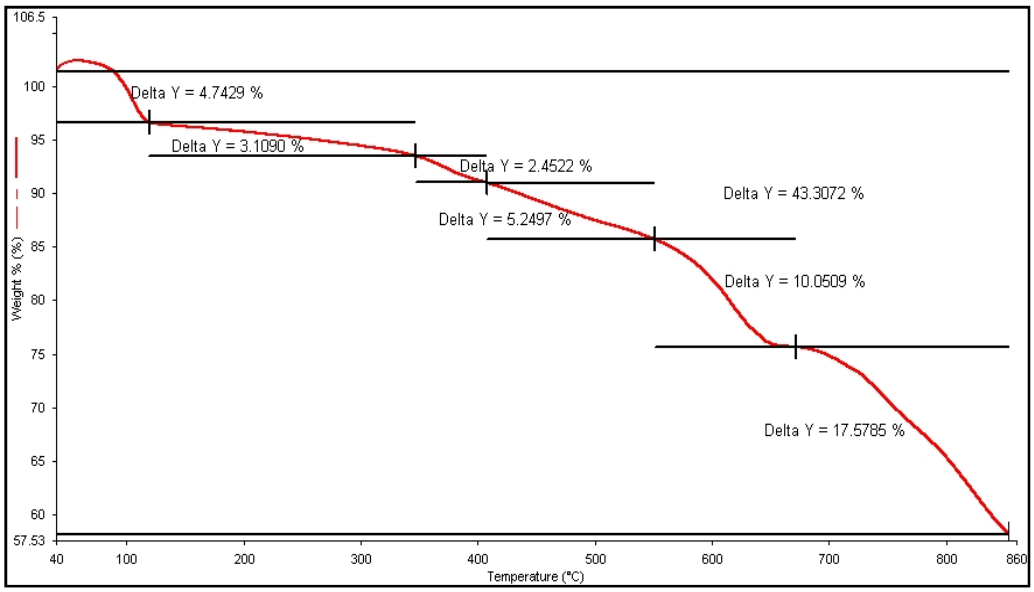

Fig. 1. TGA curve of solid material obtained after dehydration of filtrate containing $Li_4Fe(CN)_6$

sintering, contains [Fe(CN)6]4- group and hence iron is present in Fe2+ state. This was further confirmed from the UV-Vis data of commercial $K_3Fe(CN)_6$ shown in Fig. 2 (BDH, USA, 99%) [41,42]. Since no peak position of the synthesized material match with the potassium ferricyanide peaks, the synthesized materials is free from ferricyanide impurity.

3.3 Fourier Transform Infrared (FTIR) Spectroscopy

The FTIR spectrum of $Li_4Fe(CN)_6$ crystal shown in Fig. 3, detects two bands in the region of ν_{C-N}. These bands are centered at 2044 and 2071 cm^{-1}, which is due to stretching of C-N bond in $Fe(CN)_6^4$. The peaks at 552 $cm^{-1}$and 419 cm^{-1} are due to the stretching of Fe-CΞN and Fe-C, respectively, which matches well with the literature data [43-46]. The FTIR data of $K_4Fe(CN)_6$, $K_4Fe(CN)_6.3H_2O$ and $K_3Fe(CN)_6$, shown in Fig. 3, are compared with $Li_4Fe(CN)_6$ and thus confirmed the presence of ferrocyanide group.

3.4 Powder X-ray Diffraction (XRD)

The powder XRD pattern of (a) $K_4Fe(CN)_6.3H_2O$, (b) $K_4Fe(CN)_6$, (c) $K_3Fe(CN)_6$,(d) $KClO_4$, and (e) $Li_4Fe(CN)_6$ are shown in Fig. 4(i); and literature XRD pattern of (a) $Na_4Fe(CN)_6$, (b) $K_4Fe(CN)_6$ and (c) $Rb_4Fe(CN)_6$ is shown in Fig. 4(ii).

No regular sharp peak is observed in the XRD pattern of $Li_4Fe(CN)_6$ indicating the formation of both crystalline and amorphous phase. Since there is no literature report available on the XRD pattern of $Li_4Fe(CN)_6$, we are not able to compare with the literature data. Crystal structure shall be determined from the single crystal data, which is under investigation and may be reported later.

However, we have compared the XRD pattern of $Li_4Fe(CN)_6$ with the XRD pattern of $K_4Fe(CN)_6.3H_2O$, $K_4Fe(CN)_6$, $K_3Fe(CN)_6$ and $KClO_4$; and found no similarity. This indicates that the material is free from starting materials and the byproduct.

Besides this, it is an important observable thing that there are no similarities in peak positions among $Na_4Fe(CN)_6$, $K_4Fe(CN)_6$ and $Rb_4Fe(CN)_6$ Fig. 4(ii). $Li_4Fe(CN)_6$ alsodoes not show any similarities with them.

3.5 Scanning Electron Microscopy (SEM)

The surface morphology, porosity and particle size distribution of the synthesized material were studied from the SEM images, shown in Fig. 5. Particle size, shape and spaces among the particles are the key important factors to be a good cathode material. Small size particles have larger specific surface area retain higher specific capacity, because the reactions basically occur on the surface of the material. On the other hand, if the spaces among the particles are large enough to penetrate the electrolyte on the material surface, cell shows better performance.

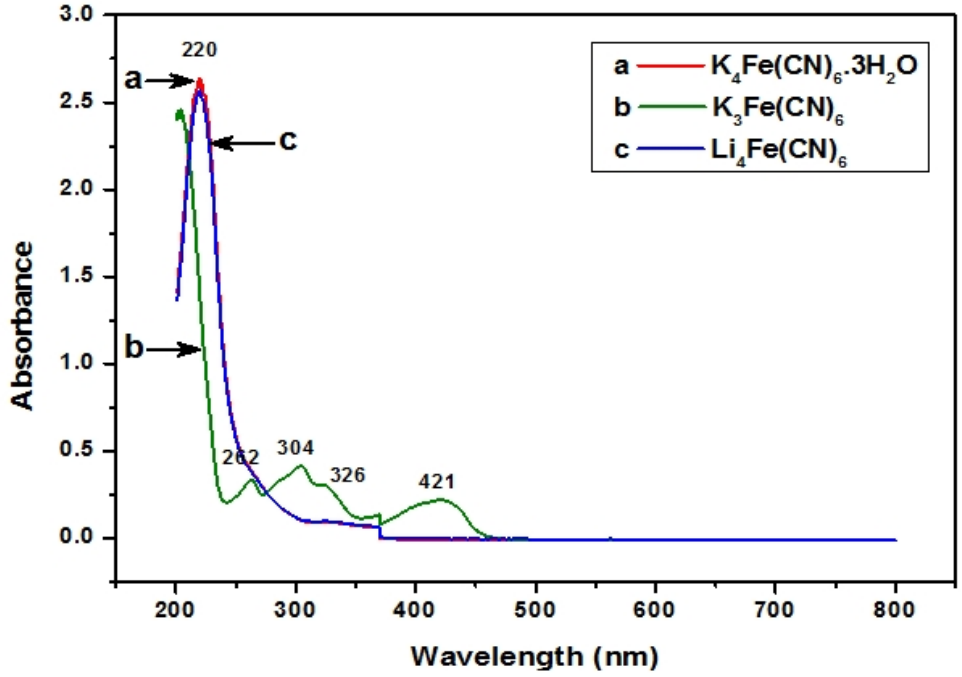

Fig. 2. UV-Visible spectrum of (a) $K_4Fe(CN)_6.3H_2O$, (b) $K_3Fe(CN)_6$ and (c) $Li_4Fe(CN)_6$

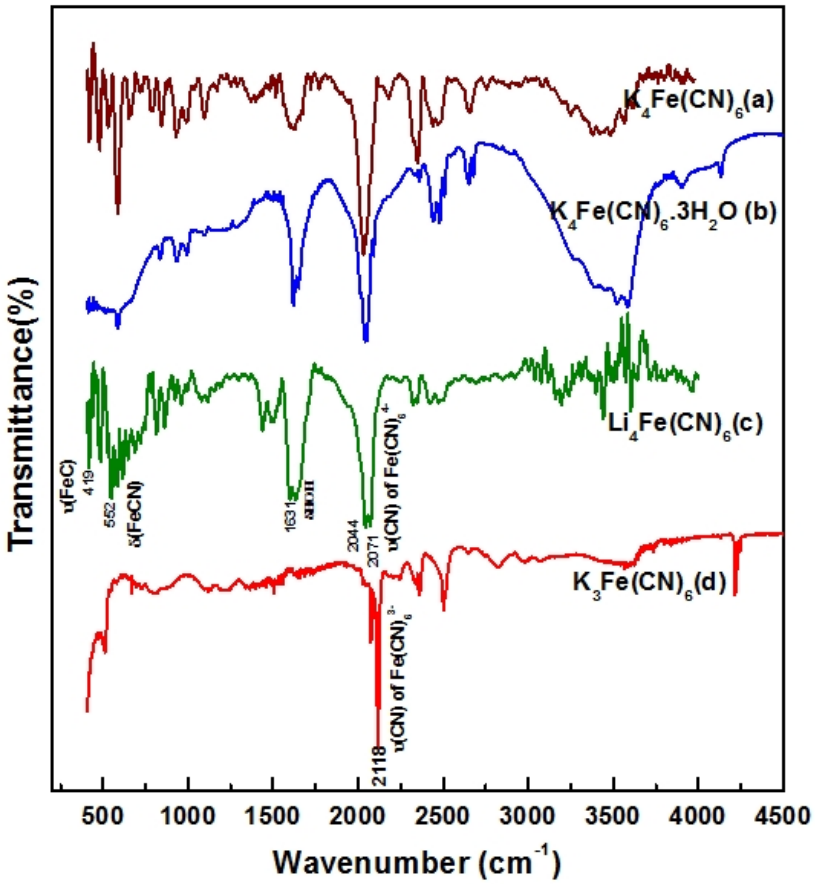

Fig. 3. FTIR spectra of (a) $K_4Fe(CN)_6$, (b) $K_4Fe(CN)_6.3H_2O$, (c) $Li_4Fe(CN)_6$ and (d) $K_3Fe(CN)_6$

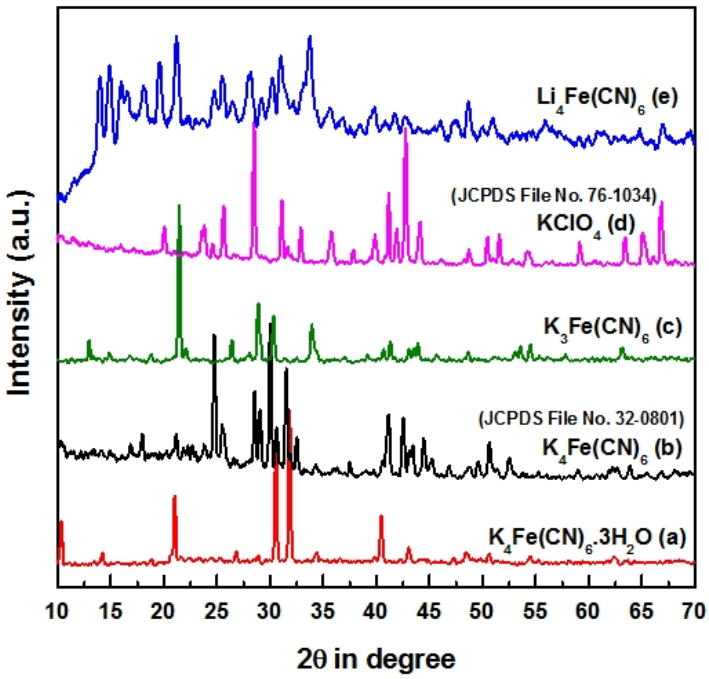

Fig. 4i. Powder XRD pattern of (a) $K_4Fe(CN)_6.3H_2O$, (b) $K_4Fe(CN)_6$, (c) $K_3Fe(CN)_6$,(d) $KClO_4$, and (e) $Li_4Fe(CN)_6$

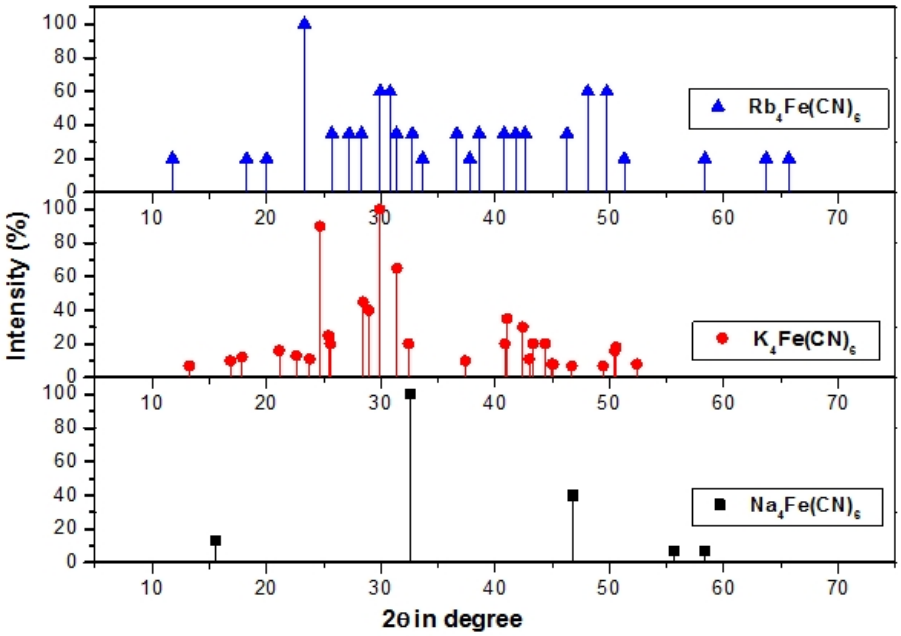

Fig. 4ii. Literature XRD pattern of (a) $Na_4Fe(CN)_6$, (b) $K_4Fe(CN)_6$ and (c) $Rb_4Fe(CN)_6$

Figs. 5a and 5b show the SEM images of the synthesized material, recorded before cell fabrication and Figs. 5c and 5d show the images after few cycles of charge-discharge. The images show that the particles are agglomerated with an average particle size varying 3-5 μm and there are no such remarkable changes in shape and sizes of the particles before and after charge-discharge process.

3.6 Energy-dispersive X-ray Spectroscopy (EDX)

EDX spectra were carried out with the material from different six regions and atomic

percentages of its constituent's elements are recorded. Fig. 6 shows the six EDX spectra and the corresponding atomic percentages of elements like K, Fe, C and N are shown in Table 1.

Li^+ cannot be detected from EDX spectra, due to its smaller size and absence of electron in higher shell than K-shell. The spectrum is generally obtained when the electron migrates from higher shell to newly created hole of K-shell. Hence, the atomic percentage of lithium atoms can only be obtained from the calculation of percentages of the other elements using the formula of $Li_xK_yFe(CN)_6$, where x+y=4. From the analysis of the six spectra and taking average value of K, Fe, C and N, shown in Table 1; we evaluate the Li atomic percentage, which results the formula of the material as $Li_{3.845}K_{0.155}Fe(CN)_6$. It is clearly indicated that about 96% of K^+ has been replaced by Li^+. The small amount of K^+ can not affect on the cell performance, because the sufficient amount of Li^+ are present for intercalation.

3.7 Electrochemical Study

The cyclic voltammogram of the synthesized $Li_4Fe(CN)_6$ cathode were recorded, as shown in Fig. 7, in the potential window of 1.5 V to 4.8 V vs. Li at a scan rate of 0.5 mVs^{-1}.

In the first cycle during forward scantwo oxidation peaks appeared at 3.58 volt and 4.4 volt and the corresponding two reduction peaks are observed at 2.71 volt and 1.75 volt. But in the next cycle, slight changes in the peak positions were observed. In the anodic scan during subsequent cycles, the peak height as well as peak area decreases at 4.4 volts by the compensation in increase in peak area at 3.21 volts. In the cathodic scan, the dual peaks converge into a single peak. This result indicates the structural changes within the molecule during oxidation-reduction process. More importantly, cyclic voltametry study reveals that the system is reversible in nature and reversibility retained in the subsequent cycles.

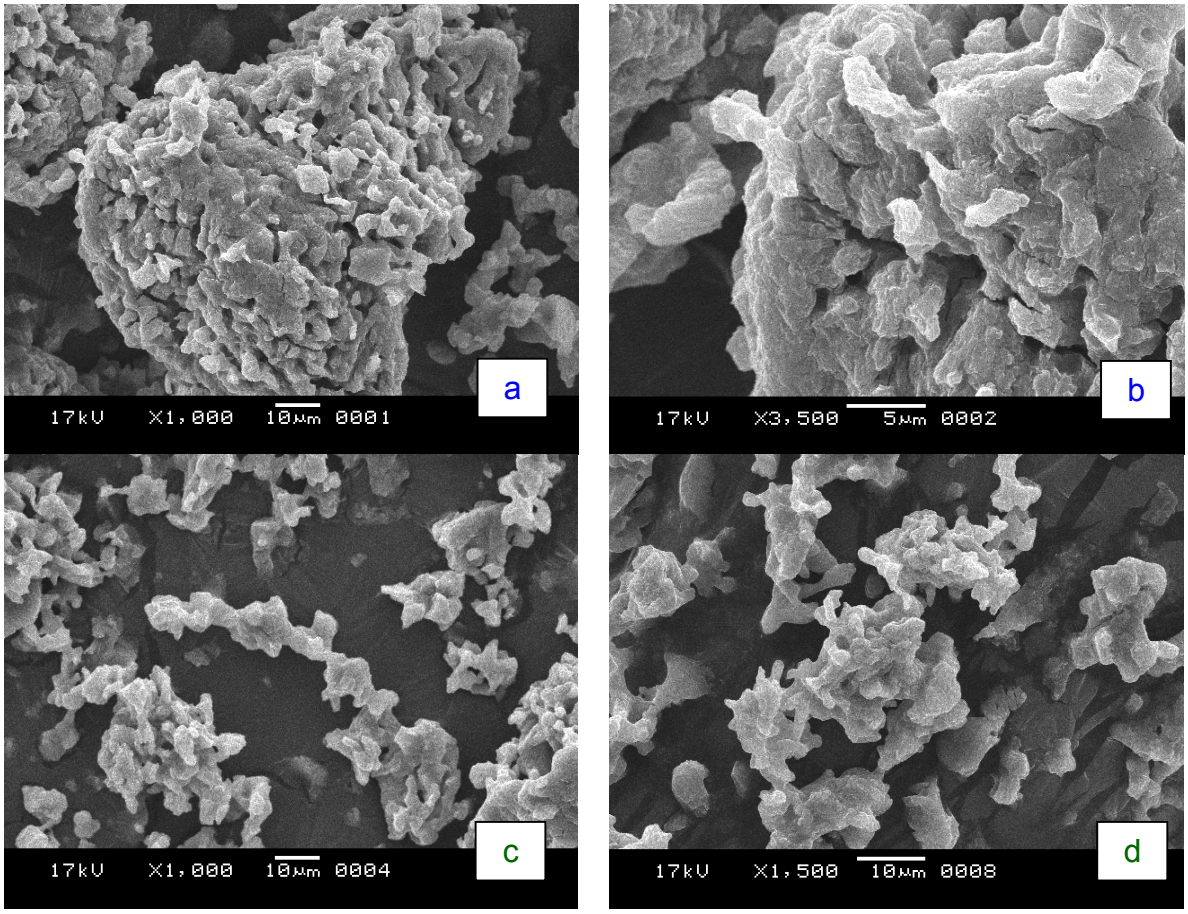

Fig. 5. SEM images of $Li_4Fe(CN)_6$ at initial state (a,b) and after few cycles charge-discharge (c,d)

Table 1. EDX data of the synthesized material showing the atomic percentage of elements viz. K, Fe, C and N

Spectrum no	Li	K	Fe	C	N	K/Fe
1		0.00	7.57	36.49	55.07	0.000
2		0.33	2.57	49.07	48.03	0.1284
3		2.44	9.51	53.62	32.66	0.2566
4		0.79	6.55	35.73	56.94	0.1206
5		2.01	9.26	49.08	37.87	0.2171
6		1.32	7.75	43.75	47.18	0.1703
	average	=1.148	=7.201	=44.623 Average C, N=45.457	=46.291	=0.159
or	3.841	0.159	1.000	6.196	6.428	
or	3.848 Formula (taking average)	0.152 $=Li_{3.845}K_{0.155}Fe(CN)_6$	0.95	6.000	6.000	

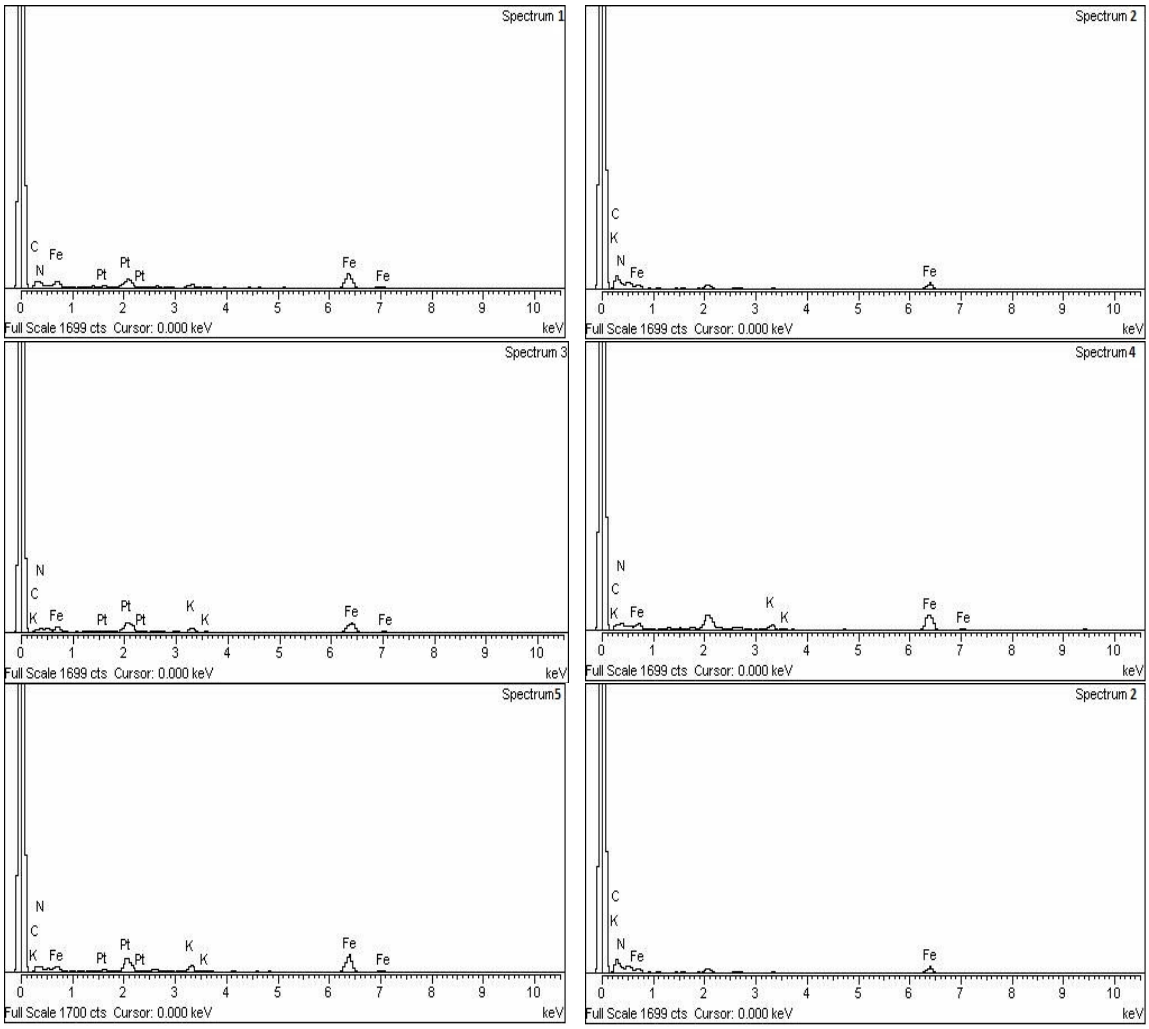

Fig. 6. EDX spectra of $Li_4Fe(CN)_6$ taken from six different regions

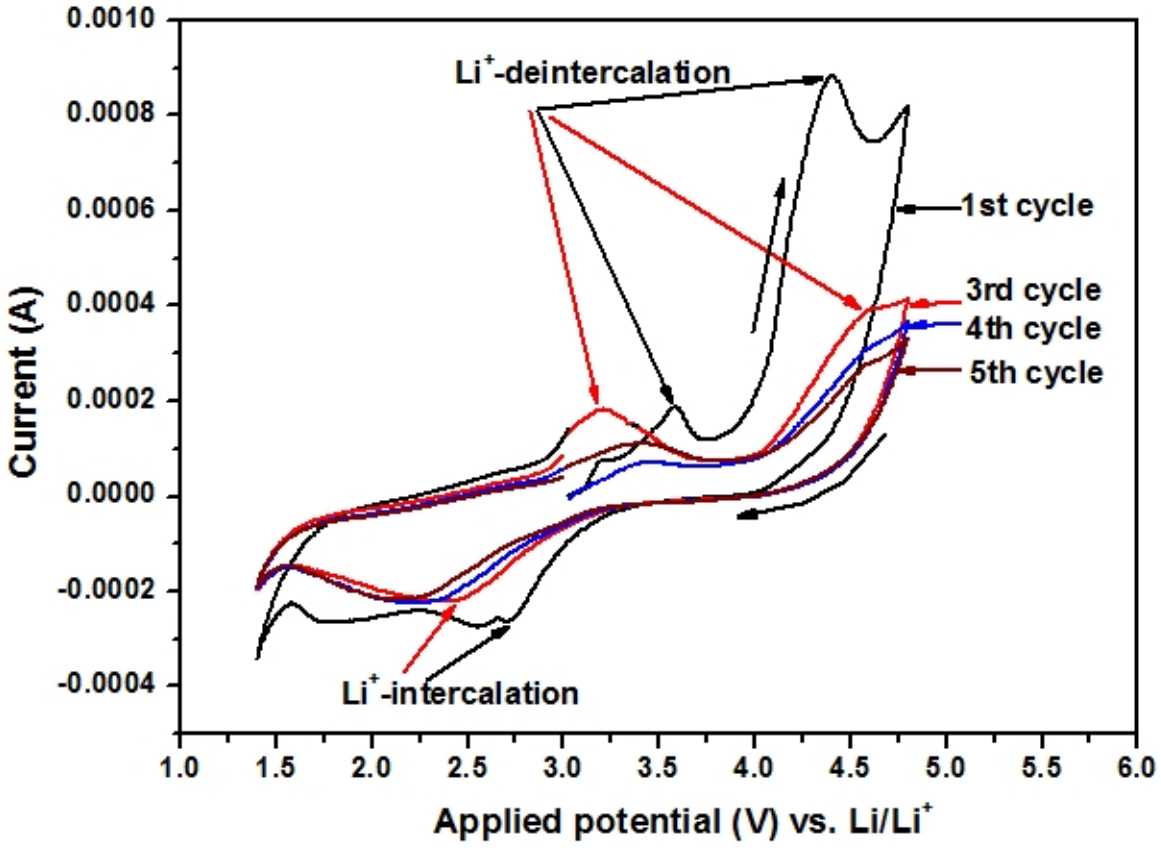

Fig. 7. Cyclic voltammogram of $Li_4Fe(CN)_6$ cathode vs. lithium anode in 1M $LiClO_4$ dissolved in 1:1 mixture of EC+DMC at the scan rate of 0.5 mVs^{-1} at 25ºC

Galvanostatic charge-discharge behaviour of the lab model cell using $Li_4Fe(CN)_6$ as cathode, shown in Fig. 8, were recorded at two different rates of 0.15 C and 0.30 C. The cell was cycled within the potential window of 1.8 V to 4.5 V vs. Li and the potential in the higher side was restricted at 4.5 V to avoid decomposition of the electrolyte.

At low rate (0.15 C), the cell shows two distinct pleato, one is at ~3.4 V and another one is at ~4.2 V during charge process. More interestingly, another pleato is shown up around 4.5 V and this might be due to removal of second lithium from the $Li_4Fe(CN)_6$ cathode, but the cut off voltage was restricted at 4.5 V to avoid electrolyte decomposition. During discharge process, two pleato are also observed, one is at ~2.7 V and another is at ~2.1 V, though they are not well distinguished. The formation of two pleato can be explained in terms of phase transition of the cyano complex. During charge process, removal of fifty percent (50%) of the first lithium from $Li_4Fe(CN)_6$ material, means fifty percent Fe^{2+} is oxidized to Fe^{3+}, cause a phase transition and thus the delithiation of the remaining fifty percent of the first lithium has taken place at higher potential. This is no doubt an interesting observation, which needs further study.

The maximum faradic capacity of 90 $mAhg^{-1}$ is obtained in a single plateau, which is about 80% of the theoretical value i.e., 112 $mAhg^{-1}$ and the value practically remain unaltered up to 15-20 cycles as shown in Fig. 9. The redox capacity retained after 20 cycles is ~94.4% of its initial value. It is interesting to see two distinct plateaus during charge process; one is at ~3.34 V and another at ~4.31 V vs. Li. This clearly suggests that the lithium ions are coming out from two different sides of the lithiated ferrocyanide complex. In other way, different energies are required to remove the lithium ions from two different sides. But lithium insertion to the host structure takes place at a single potential as observed in Fig. 8. At high drain condition the cell delivered a capacity of 37 $mAhg^{-1}$, due to migratory limitation of the Li^+ ions.

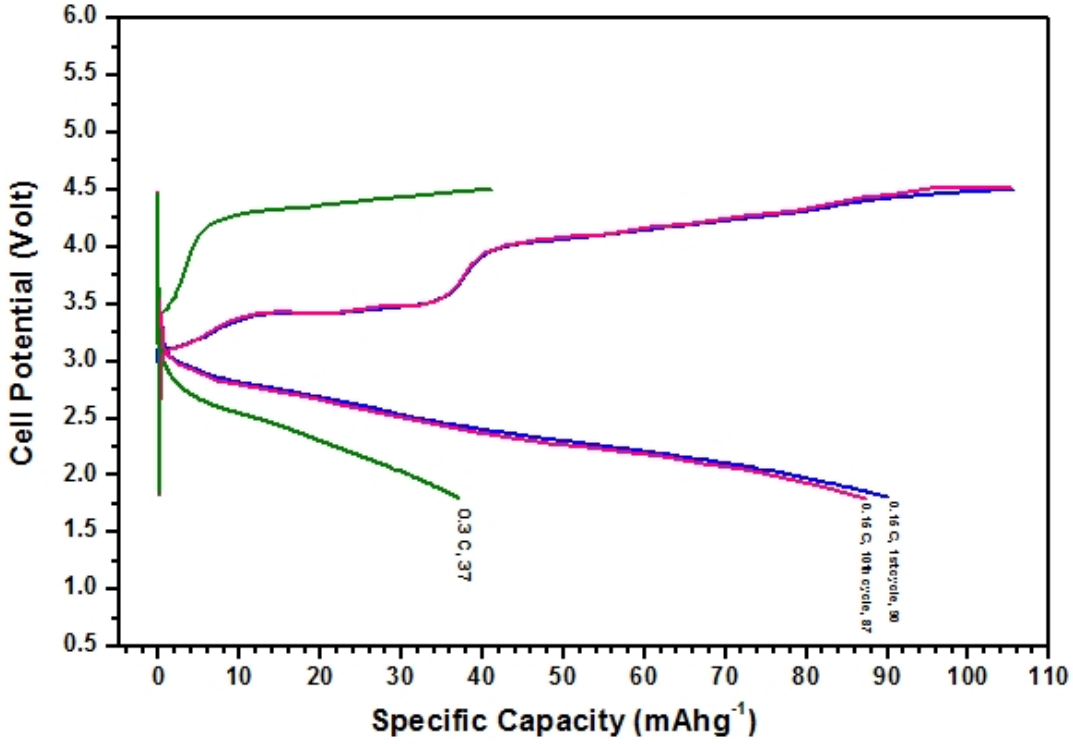

Fig. 8. Charge-discharge curve of $Li_4Fe(CN)_6$ vs. Li/Li^+ at 0.15 C and 0.30 C current densities

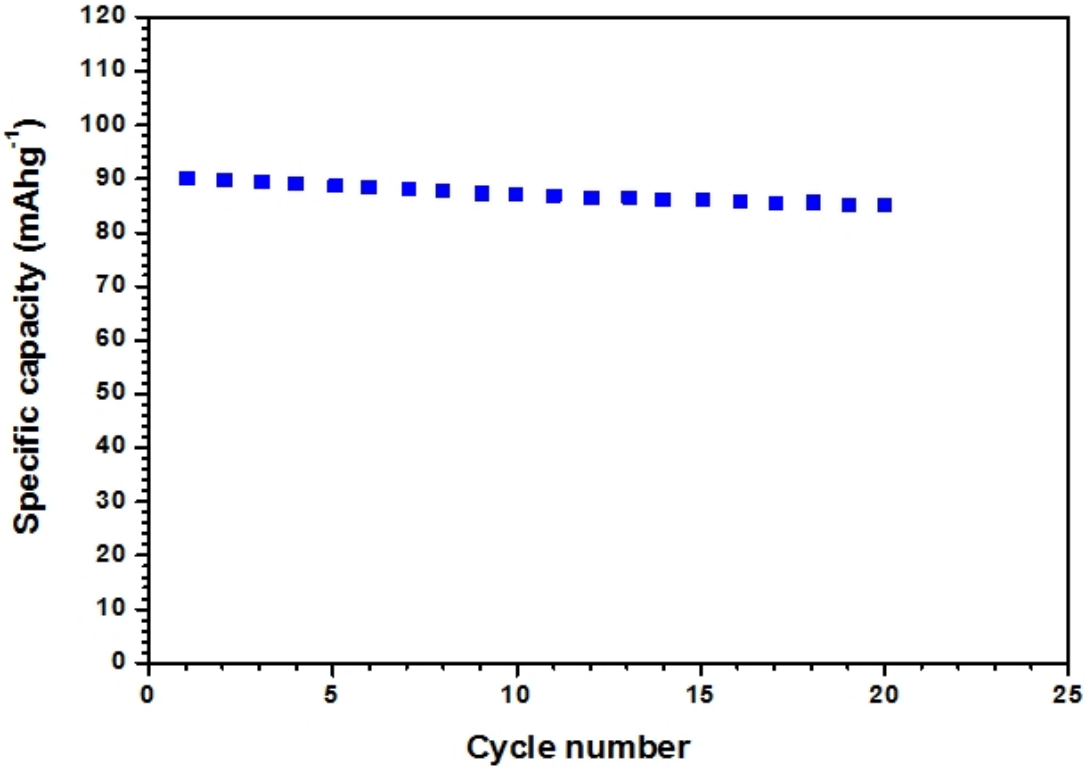

Fig. 9. Discharge capacities of $Li_4Fe(CN)_6$ cathode vs. cycle number at 0.15 C current density

4. CONCLUSION

$Li_4Fe(CN)_6$ was successfully synthesized by a simple and cost effective route. The as-prepared lithiated ferrocyanide displays a full utilization of its redox capacity of ~90 mAh g^{-1} at an average potential of 2.25 volts, an excellent cycling stability with 94.4% capacity retention over 20 cycles. Above that the advantages of this method are that no inert atmosphere and no high temperature are required during synthesis. Finally, it can be used as liquid cathode in aqueous lithium ion battery, since it is soluble in water.

COMPETING INTEREST

Authors have declared that no competing interests exist.

REFERENCES

1. Sadoway DR, Mayes AM. Portable power: Advanced rechargeable lithium batteries. MRS Bull. 2002;27:590-596.
2. Miao C, Bai P, Jiang Q, Sun S, Wang X. A novel synthesis and characterization of $LiFePO_4$ and $LiFePO_4$/C as a cathode material for lithium-ion battery. J. Power Sources. 2014;246:232-238.
3. Patil A, Patil V, Shin DW, Choi J-W, Paik D-S, Yoon S-J. Issue and challenges facing rechargeable thin film lithium batteries. Mater. Res. Bull. 2008;43:1913-1942.
4. Fergus JW. Recent developments in cathode materials for lithium ion batteries. J. Power Sources. 2010;195:939-954.
5. Liu C, Nan J, Zuo X, Xiao X, Shu D. Synthesis and electrochemical characteristics of an orthorhombic $LiMnO_2$ cathode material modified with poly (Vinyl-Pyrrolidone) for lithium Ion batteries. Int. J. Electrochem. Sci. 2012;77:7152-7164.
6. Ammundsen B, Desilvestro J, Groutso T, Hassell D, Metson JB, Regan E, Steiner R, Pickering PJ. Formation and structural properties of layered $LiMnO_2$ cathode materials. J. Electrochem. Soc. 2000;147:4078-4082.
7. Vitins G, West K. Lithium intercalation into layered $LiMnO_2$. J. Electrochem. Soc. 1997;144:2587-2592.
8. Kim DK, Muralidharan P, Lee HW, Ruffo R, Yang Y, Chan CK, Hailin P, Huggins RA, Cui Y. Spinel $LiMn_2O_4$ nanorods as lithium Ion battery cathodes. Nano Lett. 2008;8:3948–3952.
9. Zhao X, Reddy MV, Liu H, Ramakrishna S, Subba Rao GV, Chowdari BVR. Nano $LiMn_2O_4$ with spherical morphology synthesized by a molten salt method as cathodes for lithium ion batteries. RSC Adv. 2012;2:7462-7469.
10. Lee S, Cho Y, Song HK, Lee KT, Cho J. Carbon-coated single-crystal $LiMn_2O_4$ nanoparticle clusters as cathode material for high-energy and high-power lithium-Ion batteries. Angew. Chem. 2012;51:8748–8752.
11. Chen Z, Du B, Xu M, Zhu H, Li L, Wang W. Polyacene coated carbon/$LiFePO_4$ cathode for Li ion batteries: Understanding the stabilized double coating structure and enhanced lithium ion diffusion kinetics. Electrochim. Acta. 2013;109:262-268.
12. Wu G, Zhou Y, Shao Z. Carbon nanotube and graphene nanosheet co-modified $LiFePO_4$ nanoplate composite cathode material by a facile polyol process. Appl. Surf. Sci. 2013;283:999-1005.
13. Yang X, Xu Y, Zhang H, Huang Y, Jiang Q, Zhao C. Enhanced high rate and low-temperature performances of mesoporous $LiFePO_4$/Ketjen Black nanocomposite cathode material. Electrochim. Acta. 2013;114:259-264.
14. Chen TK, Qi X, Chen CY, Chang CC, Chang WC. Maleic-anhydride-grafted ketjen black as the alternative carbon additive for $LiFePO_4$ cathode. Electrochim. Acta. 2013;107:503-508.
15. Maccario M, Croguennec L, Cras F, Delmas C. Electrochemical performances in temperature for a C-containing $LiFePO_4$ composite synthesized at high temperature. J. Power Sources. 2008;183:411-417.
16. Murugan AV, Muraliganth T, Manthiram A. Rapid microwave-solvothermal synthesis of phospho-olivine nanorods and their coating with a mixed conducting polymer for lithium ion batteries. Electrochem. Commun. 2008;10:903-906.
17. Mandal B, Basumallick I, Ghosh S. One pot synthesis of Zr^{4+}doped carbon coated $LiFePO_4$ cathode material for rechargeable Li-ion battery. British J. Appl. Sci. Tech. 2014;4(10):1509-1519.
18. Wang GX, Bewlay S, Needham SA, Liu HK, Liu RS, Drozd VA, Lee JF, Chen JM. Synthesis and characterization of $LiFePO_4$ and $LiuTi_{0.01}Fe_{0.99}PO_4$ cathode

materials. J. Electrochem. Soc. 2006;153:A25-A31.
19. Chung SY, Chiang YM. Microscale measurements of the electrical conductivity of doped $LiFePO_4$. Electrochem. Solid-St. Lett. 2003;6:A278-A281.
20. Jayaprakash N, Kalaiselvi N, Periasamy P. Synthesis and characterization of $LiMXFe1-XPO_4$ (M = Cu, Sn; X = 0.02) cathodes - A study on the effect of cation substitution in $LiFePO_4$ material. Int. J. Electrochem. Sci. 2008;3:476-488.
21. Roberts MR, Spong AD, Vitins G, Owen JR. High throughput screening of the effect of carbon coating in $LiFePO_4$ electrodes. J. Electrochem. Soc. 2007;154:A921-A928.
22. Kuwahara A, Suzuki S, Miyayama M. Hydrothermal synthesis of $LiFePO_4$ with small particle size and its electrochemical properties. J. Electroceram. 2010;24:69-75.
23. Kanamura K, Koizumi S, Dokko K. Hydrothermal synthesis of $LiFePO_4$ as a cathode material for lithium batteries. J. Mater. Sci. 2008;43:2138–2142.
24. Lee J, Teja AS. Synthesis of $LiFePO_4$ micro and nanoparticles in supercritical water. Mater. Lett. 2006;60:2105–2109.
25. Kim DH, Kim J. Synthesis of $LiFePO_4$ nanoparticles and their electrochemical properties. J. Phys. Chem. Solids. 2007;68:734–737 .
26. Qin X, Wang X, Xiang H, Xie J, Li J, Zhou Y. Mechanism for hydrothermal synthesis of $LiFePO_4$ platelets as cathode material for Lithium-Ion batteries. J. Phys. Chem. C. 2010;114:16806–16812.
27. Xu Z, Xu L, Lai Q, Ji X. A PEG assisted sol–gel synthesis of $LiFePO_4$ as cathodic material for lithium ion cells. Mater. Res. Bull. 2007;42:883–891.
28. Yang J, Xu JJ. Synthesis and characterization of carbon-coated lithium transition metal phosphates $LiMPO_4$ (M = Fe, Mn, Co, Ni) prepared via a nonaqueous sol-gel route. J. Electrochem. Soc. 2006;153:716-723.
29. Lee SB, Cho SH, Cho SJ, Park GJ, Park SH, Lee YS. Synthesis of $LiFePO_4$ material with improved cycling performance under harsh conditions. Electrochem. Commun. 2008;10:1219–1221.
30. Lin Y, Pan H, Gao M, Miao H, Li S, Wang Y. Synthesis and characterization of $LiFePO_4$/C prepared via sol-gel method. Surf. Rev. Let. 2008;15:133–138.
31. Jugovic D, Mitric M, Cvjeticanin N, Janèar B, Mentus S, Uskokovic D. Synthesis and characterization of $LiFePO_4$/C composite obtained by sonochemical method. Solid St. Ionics. 2008;179:415–419.
32. Yang H, Wu XL, Cao MH, Guo YG. Solvothermal synthesis of $LiFePO_4$ hierarchically dumbbell-like microstructures by nanoplate self-assembly and their application as a cathode material in lithium-Ion batteries. J. Phys. Chem. C. 2009;113:3345–3351.
33. Recham N, Dupont L, Courty M, Djellab K, Larcher D, Armand M, Tarascon JM. Ionothermal synthesis of tailor-made $LiFePO_4$ powders for Li-Ion battery applications. Chem. Mater. 2009;21:1096-1107.
34. Beninati S, Damen L, Mastragostino M. MW-assisted synthesis of $LiFePO_4$ for high power applications. J. Power Sources. 2008;180:875–879.
35. Qian J, Zhou M, Cao Y, Ai X, Yang H. Nanosized $Na_4Fe(CN)_6$/C composite as a low-cost and high-rate cathode material for sodium-Ion batteries. Adv. Energy Mater. 2012;2:410–414.
36. [Wikipedia]. Available: http://en.wikipedia.org/wiki/Potassium ferrocyanide.
37. Wang X, Hou Y, Zhu Y, Wu Y, Holze R. An aqueous rechargeable lithium battery using coated Li metal as anode. Sci. Rep. 2013;3:1401. DOI: 10.1038/srep01401,1-5.
38. [Wikipedia]. Available: http://en.wikipedia.org/wiki/KClO4.
39. Kwon NH. The effect of carbon morphology on the LiCoO2 cathode of lithium ion batteries. Solid St. Sci. 2013;21:59-65.
40. Chen YH, Wang CW, Liu G, Song XY, Battaglia VS, Sastrya AM. Selection of conductive additives in Li-Ion battery cathodes a numerical study. J. Electrochem. Soc. 2007;154:978-986.
41. Harish S, Joseph J, Phani KLN. Interaction between gold (III) chloride and potassium hexacyanoferrate (II/III)—Does it lead to gold analogue of Prussian blue? Electrochim. Acta. 2011;56:5717–5721.
42. Chakrabarty MH, Roberts EPL. Analysis of mixtures of ferrocyanide and ferricyanide using UV-visible spectroscopy for characterisation of a novel redox flow battery. J. Chem. Soc. Pak. 2008;30(6):817-823.
43. Hussain S, Betsch K, LaCroix C. Available: http://ed.augie.edu/~calacroi/irramanlab.html.

44. Klyuev YA. Vibrational spectra of crystalline potassium ferri- and ferrocyanide. J. Appl. Spectrosc. 1965;3:30-34.
45. Idemura S, Suzuki E, Ono Y. Electronic state of iron complexes in the interlayer of hydrotalcite-like materials. Clays Clay Miner. 1989;37:553-557.
46. Balmaseda J, Reguera E, Fernandez J, Gordillo A, Yee-Madeira H. Behavior of prussian blue-based materials in presence of ammonia. J. Phys. Chem. Solid. 2003;64:685–693.

Peer-review history:
The peer review history for this paper can be accessed here:
http://www.sciencedomain.org/review-history.php?iid=650&id=7&aid=6397